

Full Structure Assignments of Pyrrolizidine Alkaloid DNA Adducts and Mechanism of Tumor Initiation

Yuewei Zhao,[†] Qingsu Xia,[†] Gonçalo Gamboa da Costa,[†] Hongtao Yu,[‡] Lining Cai,[§] and Peter P. Fu^{*,†}

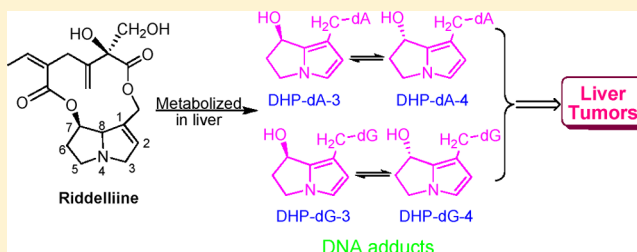
[†]National Center for Toxicological Research, Jefferson, Arkansas 72079, United States

[‡]Department of Chemistry and Biochemistry, Jackson State University, Jackson, Mississippi 39217, United States

[§]Biotranex LLC, Monmouth Junction, New Jersey 08852, United States

Supporting Information

ABSTRACT: Pyrrolizidine alkaloid-containing plants are widespread in the world and are probably the most common poisonous plants affecting livestock, wildlife, and humans. Pyrrolizidine alkaloids are among the first chemical carcinogens identified in plants. Previously, we determined that metabolism of pyrrolizidine alkaloids in vivo and in vitro generated a common set of DNA adducts that are responsible for tumor induction. Using LC-ESI/MS/MS analysis, we previously determined that four DNA adducts (DHP-dG-3, DHP-dG-4, DHP-dA-3, and DHP-dA-4) were formed in rats dosed with riddelliine, a tumorigenic pyrrolizidine alkaloid. Because of the lack of an adequate amount of authentic standards, the structures of DHP-dA-3 and DHP-dA-4 were not elucidated, and the structural assignment for DHP-dG-4 warranted further validation. In this study, we developed an improved synthetic methodology for these DNA adducts, enabling their full structural elucidation by mass spectrometry and NMR spectroscopy. We determined that DHP-dA-3 and DHP-dA-4 are a pair of epimers of 7-hydroxy-9-(deoxyadenosin-*N*⁶-yl) dehydrosupinidine, while DHP-dG-4 is 7-hydroxy-9-(deoxyguanosin-*N*²-yl) dehydrosupinidine, an epimer of DHP-dG-3. With the structures of these DNA adducts unequivocally elucidated, we conclude that cellular DNA preferentially binds dehydropyrrolizidine alkaloid, for example, dehydriddelliine, at the C9 position of the necine base, rather than at the C7 position. We also determined that DHP-dA-3 and DHP-dA-4, as well as DHP-dG-3 and DHP-dG-4, are interconvertible. This study represents the first report with detailed structural assignments of the DNA adducts that are responsible for pyrrolizidine alkaloid tumor induction on the molecular level. A mechanism of tumor initiation by pyrrolizidine alkaloids is consequently fully determined.



INTRODUCTION

Pyrrolizidine alkaloids and pyrrolizidine alkaloid *N*-oxides are common constituents of hundreds of plant species of different unrelated botanical families distributed in many geographical regions of the world.^{1–10} More than 660 pyrrolizidine alkaloids and pyrrolizidine alkaloid *N*-oxides have been identified in over 6000 plants, and about half of them exhibit hepatotoxic activity.^{1,6–8} It has been reported that about 3% of the world's flowering plants contain toxic pyrrolizidine alkaloids.¹⁰ It is highly possible that pyrrolizidine alkaloid-containing plants are the most common poisonous plants affecting livestock, wildlife, and humans.^{3,6,11–14}

Pyrrolizidine alkaloids are among the first chemical carcinogens identified in plants. In 1950, Cook et al.¹⁵ reported that rats treated with alkaloids of *Senecio jacobea* developed liver tumors. In 1954, retrorsine, a pyrrolizidine alkaloid, was found to induce liver tumors in rats.¹⁶ Since then, although extensive studies on liver tumor formation induced by pyrrolizidine alkaloids spanned over nearly half a century, the elucidation of the mechanism by which pyrrolizidine alkaloids induce tumors failed. It was not until 2001 that we found that riddelliine, a tumorigenic pyrrolizidine alkaloid, induces liver tumors through a genotoxic mechanism mediated by (±)-6,7-dihydro-7-

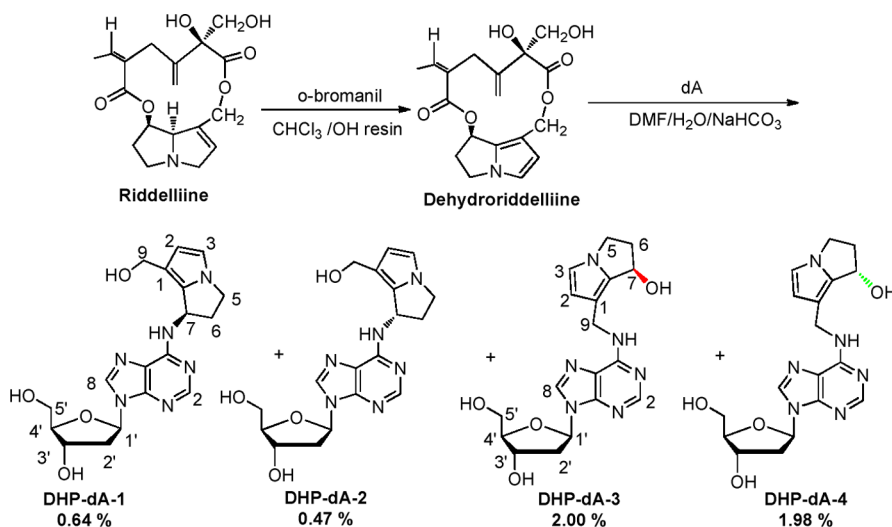
hydroxy-1-hydroxymethyl-5*H*-pyrrolizine (DHP)-derived DNA adduct formation.¹⁷ The levels of the DHP-derived DNA adducts correlated closely with tumorigenic potencies in mice fed different doses of riddelliine.^{17–19} The metabolism of riddelliine by human liver microsomes resulted in a metabolic pattern and DNA adduct profile highly similar to those formed in rat liver, indicating that the results of mechanistic studies with experimental rodents are highly relevant to humans.²⁰ These overall results suggest that riddelliine can be genotoxic to humans via DHP-derived DNA adduct formation.¹⁷ On the basis of the results of human exposure,¹³ tumor potency in experimental rodents,²¹ and mechanistic findings on riddelliine, the U.S. National Toxicology Program (NTP) classified riddelliine as “reasonably anticipated to be a human carcinogen” in the NTP 12th Report of Carcinogens.²²

Subsequent mechanistic studies on a series of different types of the pure tumorigenic pyrrolizidine alkaloids, Chinese herbal plants, and herbal dietary supplements confirmed that under similar experimental conditions, the same DHP-derived DNA adducts were generated in vivo and/or in vitro.^{23–30} The

Received: June 27, 2012

Published: August 2, 2012

Scheme 1. Synthesis of DHP-dA Adducts from Reaction of Dehydroriddelliine and dA



formation of the same DHP-derived DNA adducts from all of these studies indicates that the DHP-derived DNA adducts are potential biomarkers of pyrrolizidine alkaloid exposure and tumorigenicity.^{3,26}

The identification and quantification of these DHP-derived DNA adducts were accomplished by the ³²P-postlabeling/HPLC method.^{18,31} There are several limitations associated with ³²P-postlabeling/HPLC methods for DNA adduct analysis, in particular the lack of structural information about the DNA adducts. Subsequently, we developed an LC-ESI/MS/MS methodology for identification and quantitation of DHP-derived DNA adducts in vivo and in vitro.¹ The DHP-dG and DHP-dA synthetic standards used for HPLC-ESI-MS/MS analysis were prepared by reaction of dehydroretronecine (DHR) with dG and dA, respectively. Reaction of DHR and dG resulted in four DHP-dG adducts: an epimeric pair of 7-(deoxyguanosin-*N*²-yl)dehydrosupinidine (DHP-dG-1 and DHP-dG-2), 7-hydroxy-9-(deoxyguanosin-*N*²-yl)dehydrosupinidine (DHP-dG-3), and 7-hydroxy-5-(deoxyguanosin-*N*²-yl)dehydrosupinidine (DHP-dG-4). Reaction of DHR and dA resulted in four DHP-dA adducts: an epimeric pair of 7-(deoxyadenosin-*N*⁶-yl)dehydrosupinidine (DHP-dA-1 and DHP-dA-2) and two DHP-dA adducts tentatively assigned as x-(deoxyadenosin-*N*⁶-yl)dehydrosupinidine (DHP-dA-3), and y-(deoxyadenosin-*N*⁶-yl)dehydrosupinidine (DHP-dA-4), respectively.¹

With these synthetic standards available, the DNA adducts formed in vitro and in vivo were analyzed. We found that reaction of calf thymus DNA and DHR generated all of the four DHP-dG and four DHP-dA adducts, with DHP-dA-3 and DHP-dA-4 being the most abundant, followed by the four DHP-dG adducts, and DHP-dA-1 and DHP-dA-2 the least abundant.¹ Two liver samples were obtained from in vivo experiments using two different time courses: (i) female F344 rats were gavaged for 3 consecutive days with riddelliine or monocrotaline and (ii) female F344 rats were treated with riddelliine for 6 months. We determined that the in vivo liver DNA samples contained only DHP-dG-3, DHP-dG-4, DHP-dA-3, and DHP-dA-4 and that they were formed in a dose-responsive manner.¹

Nevertheless, there are several features considering the mechanism of pyrrolizidine alkaloid carcinogenesis that need to

be resolved. These include (i) the structures of DHP-dA-3 and DHP-dA-4 adducts; (ii) because of a limited amount of DHP-dG-4 available, the structural assignment of DHP-dG-4 has to be validated; and (iii) whether or not other DHP-derived DNA adducts are formed in vivo and/or in vitro. To clarify these matters, alternative synthetic approaches had to be developed to provide DNA adducts in a sufficient amount for structural identification.

In this study, we report the successful preparation of DHP-dG-3, DHP-dG-4, DHP-dA-3, and DHP-dA-4 by reaction of dehydroriddelliine with dG and dA. UV-visible spectrophotometry, circular dichroism (CD) analysis, and mass spectrometric and NMR spectroscopic analyses indicated that the structures of DHP-dA-3 and DHP-dA-4 were a pair of epimers of 7-hydroxy-9-(deoxyadenosin-*N*⁶-yl)dehydrosupinidine and that the structure of DHP-dG-4 was 7-hydroxy-9-(deoxyguanosin-*N*²-yl)dehydrosupinidine instead of the previously assigned 7-hydroxy-5-(deoxyguanosin-*N*²-yl)dehydrosupinidine. We also determined that DHP-dG-3 and DHP-dG-4, as well as DHP-dA-3 and DHP-dA-4, are interconvertible.

EXPERIMENTAL PROCEDURES

Caution: Riddelliine and DHP are carcinogenic in laboratory animals. They should be handled with extreme care, using proper personal protective equipment and a well-ventilated hood.

Chemicals. *o*-Bromanil, sodium bicarbonate, magnesium chloride, calf thymus DNA (sodium salt, type I), 2'-deoxyguanosine (dG), 2'-deoxyadenosine (dA), glucose-6-phosphate, glucose-6-phosphate dehydrogenase, and nicotinamide adenine dinucleotide phosphate (NADP⁺) were purchased from the Sigma Chemical Co. (St. Louis, MO). Riddelliine was obtained from Dr. Po-Chuen Chan, NTP. Alkaline phosphatase was acquired from Roche Diagnostics Corporation (Indianapolis, IN). Dehydroriddelliine was prepared by oxidation of riddelliine as previously described.^{32,33} All solvents used were HPLC grade.

Synthesis of DHP-dA Adducts. The synthesis involved the reaction of dehydroriddelliine with dA (Scheme 1). Briefly, a solution of dehydroriddelliine (10 mg, 28.7 μmol), dA (21.6 mg, 86 μmol), and NaHCO₃ (60 mg, 714 μmol) in 3 mL of DMF was reacted with stirring at 25 °C for 1 h. Deionized water (0.3 mL) was added dropwise, and the resulting solution was kept stirring for another 6 h. The reaction was quenched with deionized water (1.7 mL), and products were separated by HPLC, first with a Whatman ODS-3 column to remove excess dA and then with a Phenomenex C18 Luna

5 μm ODS column (250 mm \times 4.6 mm) eluted at 1 mL/min; elution conditions: 0–5 min, 10% acetonitrile in water; 5–50 min, 10–18% acetonitrile in water.

Synthesis of DHP-dG Adducts. Into 3 mL of anhydrous DMF in a 10 mL round-bottom flask, dehydroriddelliine (10 mg, 28.7 μmol), dG (24.4 mg, 91.5 μmol), and NaHCO_3 (60 mg, 714 μmol) were added, and the solution was stirred at room temperature for 1 h. Subsequently, 0.3 mL of deionized water was introduced dropwise into the solution under stirring. Six hours later, 1.7 mL of deionized water was added into the reaction mixture, and the solution became clear. The reaction was monitored by HPLC using a Luna C18 (2) column (250 mm \times 4.6 mm, 5 μm , Phenomenex, Torrance, CA); flow rate, 1 mL/min, monitored at 256 nm; gradient: 0–5 min, 8% acetonitrile in water; 5–50 min, 8–16% acetonitrile in water.

Interconversion between DHP-dA-3 and DHP-dA-4. Approximately 0.5 mL of a solution of pure DHP-dA-3 or DHP-dA-4 in acetonitrile/ H_2O (v/v, 1/10) in a small vial was kept at room temperature. This solution was monitored by HPLC at 0, 1, 2, 3, 4, 5, and 6 days. The percentage of DHP-dA-3 and DHP-dA-4 was calculated from the ratio of their respective peak areas relative to the sum of their peak areas. The sum of peak areas was stable ($\pm 3\%$) over the incubation period, and no additional new peaks were found during the HPLC analysis, which indicates that these two adducts were relatively stable under these conditions.

HPLC conditions: ACE C18 AR column from Mac-Mod analytical, Inc., PA, 4.6 mm \times 250 mm, 5 μm , monitored at 268 nm, with a flow rate of 1 mL/min; gradient program: 0–5 min, 10% acetonitrile in water; 5–50 min, 10–18% acetonitrile in water.

For mechanistic study, pure DHP-dA-3 in acetonitrile/ H_2O^{18} (v/v, 1/10) was similarly conducted at room temperature for a period of 6 days. The resulting DHP-dA-4 adduct was collected by HPLC for LC/MS analysis.

Interconversion between DHP-dG-3 and DHP-dG-4. Approximately 0.5 mL of a solution (acetonitrile/ H_2O = 1/10) containing pure DHP-dG-3 (or DHP-dG-4) was placed in a small vial sealed with parafilm and kept at room temperature. The solution was monitored by HPLC at 0, 1, 2, 3, 4, 5, 6, and 9 days. The analyses were then conducted under conditions described above for the interconversion between DHP-dA-3 and DHP-dA-4.

In a separate experiment, pure DHP-dG-3 in acetonitrile/ H_2O^{18} (v/v, 1/10) was similarly conducted at room temperature for a period of 8 days. The resulting DHP-dG-4 adduct was collected by HPLC for LC/MS analysis.

Metabolism of Riddelliine by Rat Liver Microsomes in the Presence of Calf Thymus DNA. The metabolism of riddelliine by male Fischer 344 rat liver microsomes was conducted in a 1.0 mL incubation volume containing 100 mM sodium phosphate buffer (pH 7.6), 5 mM magnesium chloride, 1 mM NADP^+ , 8 mM glucose 6-phosphate, 2 units of glucose 6-phosphate dehydrogenase, 0.5 mM riddelliine, 0.5 mg of purified calf thymus DNA, and 0.5 mg of microsomal protein at 37 $^\circ\text{C}$ for 60 min. After incubation, the reaction was terminated by cooling with ice-water, then sequentially extracted with 1.0 mL of phenol, 1.0 mL of phenol/chloroform/isoamyl alcohol (v/v/v, 25/24/1), and 1.0 mL of chloroform/isoamyl alcohol (v/v, 24/1). The DNA in the aqueous phase was precipitated by adding 0.1 mL of 5 M sodium chloride followed by 2 volumes of cold ethanol and washed three times with 70% ethanol. After this was redissolved in 300 μL of distilled water, the DNA concentration and purity were analyzed spectrophotometrically, and DNA was stored at -78 $^\circ\text{C}$ prior to LC/MS analysis.

DNA samples (typically ~ 100 μg) were then enzymatically hydrolyzed to deoxynucleosides with micrococcal nuclease (MN), spleen phosphodiesterase (SPD), and nuclease P1 as previously described.⁴ The resulting samples were injected on the HPLC for LC-ESI/MS/MS analyses.

LC-MS/MS Analysis of DHP-dG and DHP-dA Adducts Formed from Organic Synthesis and from Metabolism of Riddelliine by Male Fischer 344 Rat Liver Microsomes in the Presence of Calf Thymus DNA. The DHP-dG and DHP-dA adducts formed from the synthetic reactions were dissolved in water

for LC-MS/MS analysis. For those from metabolism, after enzymatic hydrolysis of the resulting reaction, the sample was dried by lyophilization. The residue was reconstructed with 100 μL of water. The reconstituted sample was qualitatively analyzed on an LC-MS/MS system.

The liquid chromatography system consisted of a Shimadzu Prominence HPLC system, including a CBM-20A system controller, two LC-20AD pump, a SIL-20AC HT autosampler, and a SPD-20A UV/vis detector (Shimadzu Scientific Instrument, Columbia, MD) and an automated switching valve (TPMV, Rheodyne, Cotati, CA). The switching valve was used to divert the column effluent to either waste or a MS instrument. The Shimadzu Prominence HPLC system was used for sample injection and separation. Each sample (10–30 μL) was loaded onto a reverse phase column [Ace 3 C18, 2.1 mm \times 100 mm, 3 μm , MAC-MOD Analytical, Chadds Ford, PA] with a water/acetonitrile gradient at 0.2 mL/min, and the sample components were eluted into the mass spectrometer. The column chamber's temperature was set to 45 $^\circ\text{C}$. The mobile phases were water and acetonitrile. The initial gradient consisted of 0% acetonitrile for 0.5 min followed by a linear gradient up to 15% acetonitrile over 50 min, and acetonitrile was increased to 95% in 1.5 min. After holding 95% acetonitrile for 5 min, the instrument was reset to the initial conditions in 1 min. The analytical column was equilibrated with the starting mobile phase for 12 min. The total run time for analysis was 70 min.

The HPLC elute was coupled with an AB Sciex 4000 QTrap LC/MS/MS system (AB Sciex, Foster City, CA), equipped with a Turbo V ion source and a desolvation temperature of 500 $^\circ\text{C}$. Nitrogen was used as the curtain gas, nebulizer gas, heater gas, and collision gas. The samples were acquired in positive IonSpray mode using multiple reaction monitoring methods (MRM). The ion transitions of the MRM method for specific detection of DHP-dG and DHP-dA adducts in the samples were m/z 403/269 and m/z 387/253, respectively. The IonSpray Voltage was 4000 V; the ion source gas 1 and gas 2 were set to 60 and 50, respectively. The declustering potential was 50 V, and the collision energy was 19 eV for all of the transitions.

High-Resolution Mass Spectral Data. The samples were analyzed on an Agilent Technologies Zorbax C8 column (4.6 mm \times 150 mm), 5 μm on a Shimadzu 20 series LC system with two mobile phases: A, H_2O containing 0.1% formic acid, and B, acetonitrile; eluted with A for 5 min, then increased from A to 35% B in A in 30 min; flow rate, 0.7 mL/min. This HPLC system was coupled with an LTQ Orbitrap mass spectrometer from Thermo Corporation (Waltham, MA), operated at a resolution of 15000.

Instrumentation. A Waters HPLC system, consisting of a model 600 controller, a model 996 photodiode array detector, and a 600 pump, was used for separation and purification of the DHP-derived DNA adducts. ^1H NMR experiments were carried out at 301 K on a Bruker Avance III spectrometer equipped with a Bruker BBFO Plus Smart Probe (Bruker Instruments, Billerica, MA) operating at 500 MHz. Samples were dissolved in $\text{DMSO-}d_6$ or $\text{DMSO-}d_6$ with a trace of D_2O . Chemical shifts are reported in parts per million downfield from tetramethylsilane, and coupling constants are reported in hertz. Two-dimensional NMR homonuclear decoupling (COSY) and NOE difference (NOESY) experiments were conducted to assist in assigning proton resonances. CD spectra were recorded on a J-500A Spectropolarimeter (Japan Spectroscopic Co. Ltd.).

RESULTS

Synthesis of DHP-dA Adducts. We previously reported that the reaction of DHR with dA generated DHP-dA-1, DHP-dA-2, DHP-dA-3, and DHP-dA-4 adducts; the yields of these adducts were only 0.1, 0.1, 0.01, and 0.01%, respectively. In the present study, the synthesis of DHP-dA adducts was attempted by reaction of dehydroriddelliine with dA under several different experimental conditions. The condition that provided the optimal yields was a reaction of dehydroriddelliine with dA in the presence of NaHCO_3 in DMF at 25 $^\circ\text{C}$ for 1 h, followed by the addition of water and further reaction for another 6 h

(Scheme 1). The resulting reaction products were separated by HPLC, first with a Whatman ODS-3 column to remove excess dA (data not shown) and then with a Phenomenex C18 Luna 5 μm ODS column (Figure 1A). The materials contained in the

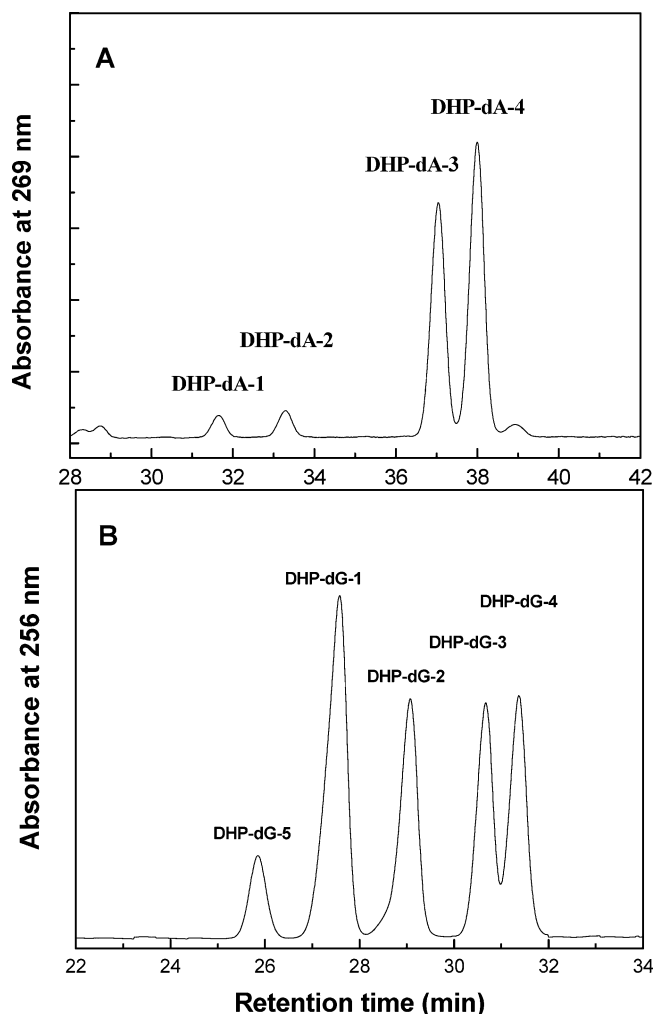


Figure 1. Reversed-phased HPLC profile of (A) DHP-dA adducts formed from reaction of dA with dehydroriddelliine using a Phenomenex C18 Luna (2) column (4.6 mm \times 250 mm, 5 μm) eluted at 1 mL/min; elution conditions: 0–5 min, 10% acetonitrile in water; 5–50 min, 10–18% acetonitrile in water; and (B) DHP-dG adducts formed from reaction of dehydroriddelliine with dG; HPLC conditions: Luna C18 (2) column (4.6 mm \times 250 mm, 5 μm); flow rate, 1 mL/min, monitored at 256 nm; gradient: 0'–5', 8% acetonitrile in water; 5'–50', 8–16% acetonitrile in water.

chromatographic peaks eluted at 31.7 and 33.3 min exhibited HPLC retention times (Figure 1A), UV–vis absorption spectra (Figure S1 in the Supporting Information), and LC/MS spectra (data now shown) identical to those of DHP-dA-1 and DHP-dA-2, respectively, previously identified as a pair of epimeric DHP-dA adducts (\pm)7-(deoxyadenosin- N^6 -yl)-dehydrosupinidine (Scheme 1) synthesized by reaction of DHR and dA.¹

High-resolution electrospray positive product ion mass spectrometric analysis revealed that the material contained in the chromatographic peaks eluting at 37.1 min (Figure 1A) had a protonated molecule ion ($M + H$)⁺ at m/z 387.1778 (calculated mass at m/z 387.1775, accuracy of 0.79 ppm) and

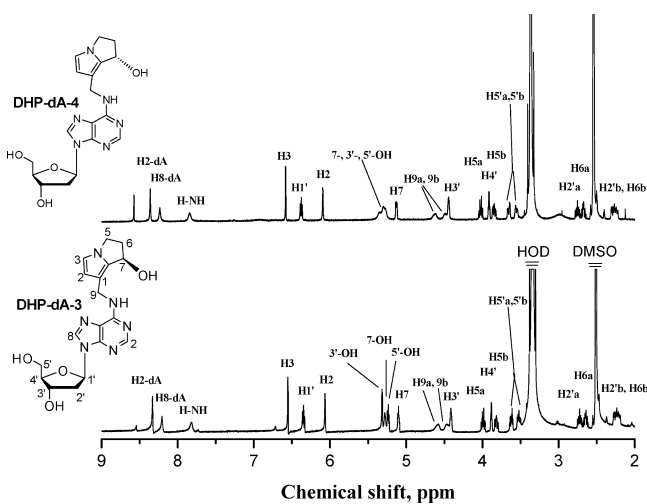
major fragments at m/z 136 (DHP-OH), 253 (loss of deoxyribose and OH), and 369 (loss of OH) (Figure S2 in the Supporting Information), suggesting that it is a DHP-derived dA adduct. This adduct had its HPLC retention time and mass spectral pattern identical to that of the adduct previously designated as DHP-dA-3 from the reaction of DHR and dA, whose structure we had previously been unable to elucidate by ¹H NMR due to an insufficient amount of sample.¹ With a sufficient quantity of this adduct, also designated here as DHP-dA-3, available from the new synthetic approach, its structure was elucidated by NMR spectral analysis. This adduct had a ¹H NMR resonance for H7 (5.09–5.11 ppm) of the DHP moiety (the necine base) that was nearly identical to H7 (4.99 ppm) of DHR (Table 1 and Figure 2); likewise, H2, H3, and both pairs of geminal H5 and H6 protons were almost unaffected by adduct formation. The full ¹H NMR spectral assignments are as follows. DHP-dA-3: ¹H NMR (DMSO- d_6): δ 2.19–2.28 (2H, m, dA-H2'b, H6b), 2.61–2.68 (1H, m, H6a), 2.70–2.75 (1H, m, dA-H2'a), 3.50–3.54 (1H, M, dA-H5'b), 3.60–3.64 (1H, m, dA-H5'a), 3.79–3.84 (1H, m, H5b), 3.87–3.89 (1H, m, dA-H4'), 3.97–4.02 (1H, m, H5a), 4.42 (1H, m, dA-H3'), 4.46 (1H, w, H9b), 4.58 (1H, w, H9a), 5.09–5.11 (1H, m, H7), 5.22–5.32 (3H, m, dA-5'-OH, 7-OH, dA-3'-OH), 6.07 (1H, d, H2, $J = 2.5$), 6.33–6.36 (1H, t, dA-H1'), 6.55 (1H, d, H3, $J = 2.5$), 7.82 (1H, bs, dA-N6H), 8.20 (1H, bs, dA-H8), 8.33 (1H, s, dA-H2).

Each of the deoxyribose protons was clearly evident for the dA moiety. The structural assignment was further confirmed by both COSY (Figure S3 in the Supporting Information) and NOESY (Figure S4 in the Supporting Information) NMR analysis. As evidenced by the COSY and NOESY 2D NMR spectral results summarized in Figure S5 in the Supporting Information, the proton–proton interactions through the bond and space clearly confirmed that reaction occurred at C9 of dehydroriddelliine and the exocyclic nitrogen of dA. Thus, on the basis of the UV–vis, mass, and ¹H NMR spectroscopic data, DHP-dA-3 was characterized as 7-hydroxy-9-(deoxyadenosin- N^6 -yl)dehydrosupinidine (Scheme 1).

The material contained in the chromatographic peaks eluted at 37.9 min (Figure 1A) was similarly analyzed. The high-resolution electrospray positive product ion mass spectrometric analysis revealed that this adduct had an observed molecular ion at m/z 387.1779 (calculated mass at m/z 387.1775, accuracy of 1.07 ppm), and major fragments at m/z 136 (DHP-OH), 253 (loss of deoxyribose and OH), and 369 (loss of OH) (Figure S6 in the Supporting Information). Its HPLC retention time and mass spectral pattern were identical to those of the adduct previously designated as DHP-dA-4 from the reaction of DHR and dA.¹ Similar to DHP-dA-3, in our previous study, we had been unable to obtain a sufficient amount of this adduct for structural identification. The complete ¹H NMR assignment of DHP-dA-4 is as follows: ¹H NMR (DMSO- d_6): δ 2.22–2.31 (2H, m, dA-H2'b, H6b), 2.64–2.71 (1H, m, H6a), 2.73–2.78 (1H, m, dA-H2'a), 3.55–3.57 (1H, M, dA-H5'b), 3.64–3.67 (1H, m, dA-H5'a), 3.82–3.87 (1H, m, H5b), 3.90–3.92 (1H, m, dA-H4'), 4.00–4.05 (1H, m, H5a), 4.44–4.45 (1H, m, dA-H3'), 4.49 (1H, w, H9b), 4.62 (1H, w, H9a), 5.12–5.13 (1H, m, H7), 5.27–5.35 (3H, m, dA-5'-OH, 7-OH, dA-3'-OH), 6.09 (1H, d, H2, $J = 2.0$), 6.36–6.39 (1H, t, dA-H1'), 6.58 (1H, d, H3, $J = 2.0$), 7.84 (1H, bs, dA-N6H), 8.24 (1H, bs, dA-H8), 8.36 (1H, s, dA-H2). The ¹H NMR spectrum of DHP-dA-4 is similar to that of DHP-dA-3 (Table 1 and Figure 2), suggesting that it is also 7-hydroxy-9-(deoxyadenosin- N^6 -yl)-

Table 1. Proton NMR Spectroscopic Data (500 MHz) of the Necine Base in the Synthetically Prepared DHP-dA and DHP-dG Adducts Measured in DMSO-*d*₆

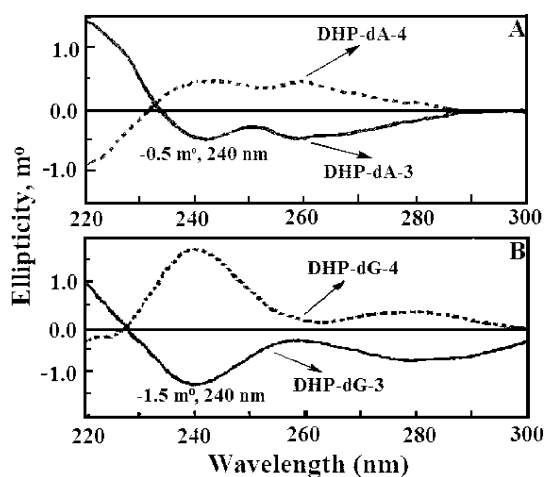
assignment	DHR ¹	adduct				
		DHP-dA-3	DHP-dA-4	DHP-dG-3	DHP-dG-4	DHP-dG-5
H6b	2.15–2.20 (1H, m)	2.19–2.28 (1H, m)	2.22–2.31 (1H, m)	2.18–2.25 (1H, m)	2.21–2.27 (1H, m)	2.15–2.24 (1H, m)
H6a	2.57–2.65 (1H, m)	2.61–2.68 (1H, m)	2.64–2.71 (1H, m)	2.55–2.66 (1H, m)	2.63–2.72 (1H, m)	2.58–2.74 (1H, m)
H5b	3.75–3.79 (1H, m)	3.79–3.84 (1H, m)	3.82–3.87 (1H, m)	3.78–3.83 (1H, m)	3.83–3.88 (1H, m)	3.78–3.84 (1H, m)
H5a	3.94–3.98 (1H, m)	3.97–4.02 (1H, m)	4.00–4.05 (1H, m)	3.98–4.03 (1H, m)	4.02–4.07 (1H, m)	3.98–4.03 (1H, m)
H9b	4.27 (1H, d, <i>J</i> = 12)	4.46 (1H, w)	4.49 (1H, w)	4.24 (1H, two sets of d, <i>J</i> = 14)	4.28 (1H, two sets of d, <i>J</i> = 14)	4.60 (1H, d, H9b, <i>J</i> = 15.5)
H9a	4.33 (1H, d, <i>J</i> = 12)	4.58 (1H, w)	4.62 (1H, w)	4.32 (1H, two sets of d)	4.37 (1H, two sets of d)	5.33 (1H, d, H9a, <i>J</i> = 15.5)
H7	4.99 (1H, dd, <i>J</i> = 6.5, 2.5)	5.09–5.11 (1H, m)	5.12–5.13 (1H, m)	5.03–5.08 (1H, m)	5.08–5.10 (1H, m)	5.20–5.22 (1H, m)
H2	6.02 (1H, d, <i>J</i> = 2.5)	6.07 (1H, d, <i>J</i> = 2.5)	6.09 (1H, d, <i>J</i> = 2.0)	6.07 (1H, d, <i>J</i> = 2.5)	6.12 (1H, d, <i>J</i> = 2.5)	5.98 (1H, d, <i>J</i> = 2.5)
H3	6.54 (1H, d, <i>J</i> = 2.6)	6.55 (1H, d, <i>J</i> = 2.5)	6.58 (1H, d, <i>J</i> = 2.0)	6.60 (1H, d, <i>J</i> = 2.5)	6.63 (1H, d, <i>J</i> = 2.5)	6.58 (1H, d, <i>J</i> = 2.5)

**Figure 2.** ¹H NMR spectra of DHP-dA-3 and DHP-dA-4 measured in DMSO-*d*₆.

dehydrosupinidine. For further structural confirmation, both COSY (Figure S7 in the Supporting Information) and NOESY (Figure S8 in the Supporting Information) spectra were obtained and analyzed. As shown in Figure S5 in the Supporting Information, the COSY and NOESY spectra of DHP-dA-4 and DHP-dA-3 are well correlated.

On the basis of the similarity of the UV spectra and assuming that the molar extinction coefficients of DHP-dA-3 and DHP-dA-4 are identical to those of DHP-dA-1 and DHP-dA-2, the reaction yields of the DHP-dA adducts from the reaction of riddelliine and dA are as follows: DHP-dA-1, 0.64%; DHP-dA-2, 0.47%; DHP-dA-3, 2.0%; and DHP-dA-4, 1.98% (Scheme 1). The yields of DHP-dA-3 and DHP-dA-4 are approximately 200-fold higher than those from the reaction of DHR and dA.

To investigate the stereochemistry, CD spectra of DHP-dA-3 and DHP-dA-4 were measured. As shown in Figure 3A, the CD Cotton effects of DHP-dA-3 were approximate mirror images of those of DHP-dA-4. It is noteworthy that the CD Cotton effects of DHP-dA-3 and DHP-dA-4 are much weaker than those of DHP-dA-1 and DHP-dA-2.¹ The overall results of UV-vis, LC/MS, 1D and 2D NMR (COSY and NOESY), and

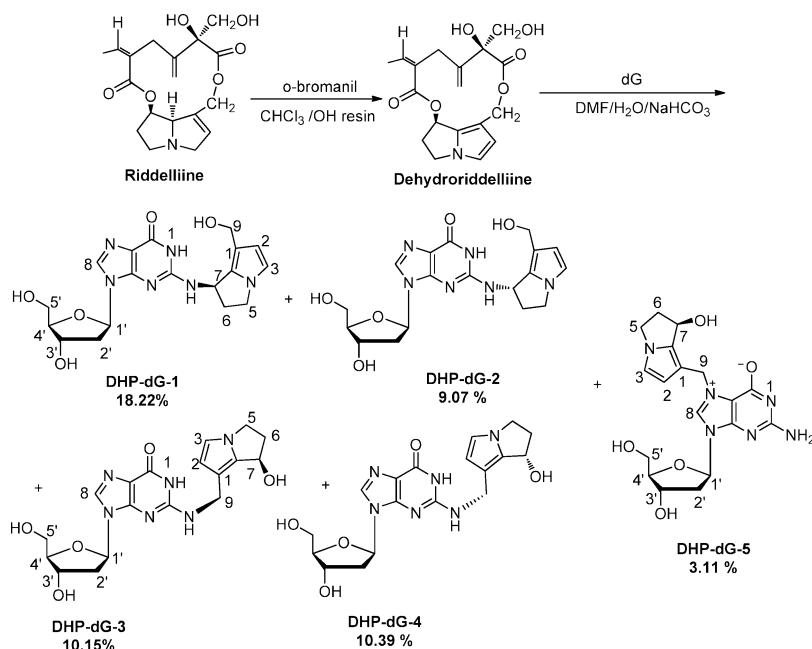
**Figure 3.** CD spectra of (A) DHP-dA-3 and DHP-dA-4, both adjusted to 1.5 OD at 270 nm, and (B) DHP-dG-3 and DHP-dG-4, both adjusted to 0.85 OD at 256 nm, in aqueous solution (acetonitrile/water = 1/10). The CD spectrometer parameters were 2 m²/cm sensitivity, 1 cm/min chart speed.

CD spectral analysis confirmed that DHP-dA-3 and DHP-dA-4 are a pair of epimers differing in the configuration of one stereocenter in the DHP chromophore (Scheme 1).

Synthesis of DHP-dG Adducts. The four DHP-dG adducts, assigned as DHP-dG-1, DHP-dG-2, DHP-dG-3, and DHP-dG-4, were previously synthesized from reaction of DHR and dG, and their structures were determined by UV-visible absorption, mass spectrometry, and ¹H NMR spectral analysis.¹ The yields of these DHP-dG adducts obtained from this reaction were DHP-dG-1, 0.89%; DHP-dG-2, 0.69%; DHP-dG-3, 0.15%; and DHP-dG-4, 0.06%, respectively.

Given that only very small amounts of DHP-dG-3 and DHP-dG-4 were previously obtained for ¹H NMR structural analysis, we felt that their structural assignments warranted validation. We have now developed an alternative synthetic method, reaction of dehydroriddelliine with dG, to obtain sufficient amounts to validate the structural assignment of these two adducts. After the DHP-dG adducts were synthesized by reaction of dehydroriddelliine with dG (Scheme 2), the

Scheme 2. Synthesis of DHP-dG Adducts from Reaction of Dehydroriddelliine with dG



resulting reaction products were separated by HPLC, first with a Whatman ODS-3 column to remove excess dG (data not shown) and then with a Phenomenex C18 Luna $5 \mu\text{m}$ ODS column (Figure 1B). The chromatographic peaks eluting at 25.8, 27.7, 29.1, 30.8, and 31.5 min (Figure 1B) had their UV-vis absorption spectra and mass spectra with identical protonated molecules ($M + H$)⁺ at m/z 403, closely similar to those previously reported for DHP-dG-1, DHP-dG-2, DHP-dG-3, and DHP-dG-4.¹ On the basis of their HPLC profile (Figure 1B), UV-visible absorption spectra, ¹H NMR spectra (data not shown), and mass spectral patterns, the chromatographic peaks eluting at 27.7, 29.1, 30.8, and 31.5 min were identified as the previously determined DHP-dG-1, DHP-dG-2, DHP-dG-3, and DHP-dG-4 adducts.¹ On the basis of ¹H NMR (Figure 4) and 2D NMR (COSY and NOESY) spectral analysis (Figure S9 and S10 in the Supporting Information), we confirmed that the structure of DHP-dG-3 is 7-hydroxy-9-

(deoxyguanosin-*N*²-yl)dehydrosupinidine. This confirms that the previous structure assignment is indeed correct. However, we determined that the full proton ¹H NMR spectrum of DHP-dG-4 adduct should be assigned as follows: DHP-dG-4: ¹H NMR ($\text{DMSO}-d_6$): δ 2.21–2.27 (2H, m, dG-H2'b, H6b), 2.63–2.72 (2H, m, dG-H2'a, H6a), 3.50–3.60 (2H, m, dG-H5'), 3.83–3.88 (2H, m, dG-H4', H5b), 4.02–4.07 (1H, m, H5a), 4.28 (1H, H9, two set of d, $J = 14$ Hz), 4.37 (1H, H9a, two set of d, $J = 14$ Hz), 4.41 (1H, m, dG-H3'), 5.03 (1H, w, OH), 5.08–5.10 (1H, m, H7), 5.34 (1H, m, OH), 6.12 (1H, d, H2, $J = 2.5$), 6.23 (1H, m, dG-H1'), 6.63 (1H, d, H3, $J = 2.5$), 7.92 (1H, s, dG-H8), 8.57 (1H, s, OH/NH), 10.72 (1H, bs, dG-NH1). On the basis of this full proton NMR assignment and the NMR data (Table 1) and shown in Figure 4, the NMR spectral data of DHP-dG-4 are similar to those of DHP-dG-3. Analysis of the COSY NMR spectrum (Figure S11 in the Supporting Information) and the NOESY NMR spectrum (Figure S12 in the Supporting Information) also indicated that the structure of the DHP-dG-4 adduct should also be 7-hydroxy-9-(deoxyguanosin-*N*²-yl)dehydrosupinidine. The CD spectra of DHP-dG-3 and DHP-dG-4 adducts (Figure 3B) further validated that they are a pair of epimeric DHP-dG adducts with the asymmetric center at the C7 position of the necine base (Scheme 2). Thus, the previous assignment of DHP-dG-4 as 7-hydroxy-5-(deoxyguanosin-*N*²-yl)dehydrosupinidine¹ is incorrect.

An additional DHP-dG adduct, assigned as 7-hydroxy-9-(deoxyguanosin-*N*⁷-yl)dehydrosupinidine (DHP-dG-5), was also obtained from this new synthetic approach (Figure 1B). Its mass spectrum had a protonated molecule ($M + H$)⁺ at m/z 403, identical to those of DHP-dG-1, DHP-dG-2, DHP-dG-3, and DHP-dG-4. On the basis of its mass, ¹H NMR (Figure 5 and Table 1), 2D COSY NMR (Figure S13 in the Supporting Information), and spectral analyses (Figure S14 in the Supporting Information), this adduct was assigned as DHP-dG-5. The proton NMR assignment of DHP-dG-5 is as follows: DHP-dG-5: ¹H NMR ($\text{DMSO}-d_6$): δ 2.15–2.24 (2H, m, dG-H2'b, H6b), 2.58–2.74 (2H, m, dG-H2'a, H6a), 3.46–3.55

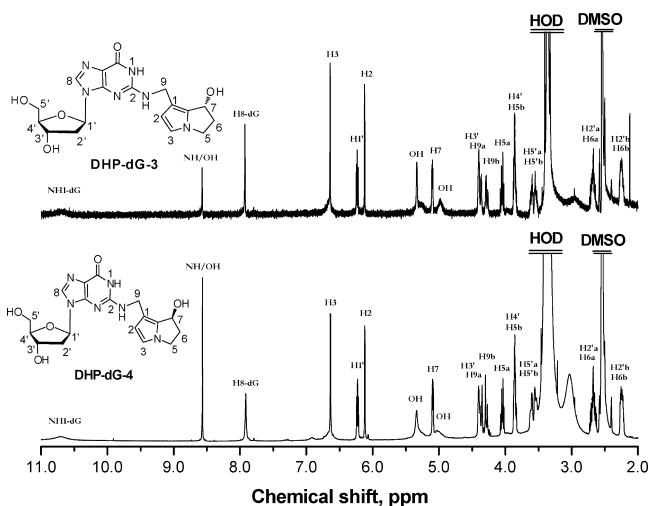


Figure 4. ¹H NMR spectra of DHP-dG-3 and DHP-dG-4 measured in $\text{DMSO}-d_6$. The absolute stereochemistries depicted at C7 are arbitrary.

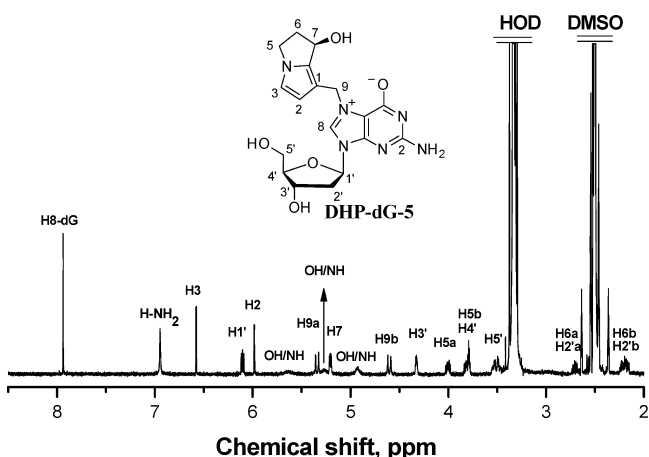


Figure 5. ^1H NMR spectra of DHP-dG-5 measured in $\text{DMSO}-d_6$.

(2H, m, dG-H5'), 3.78–3.84 (2H, m, dG-H4', H5b), 3.98–4.03 (1H, m, H5a), 4.32–4.34 (1H, m, dG-H3'), 4.60 (1H, d, H9b, $J = 15.5$), 4.93 (1H, w, NH/OH), 5.20–5.22 (1H, m, H7), 5.28 (1H, w, NH/OH), 5.33 (1H, d, H9a, $J = 15.5$), 5.63 (1H, w, NH/OH), 5.98 (1H, d, H2, $J = 2.5$), 6.09–6.12 (1H, m, dG-H1'), 6.58 (1H, d, H3, $J = 2.5$), 6.95 (2H, b, NH_2), 7.94 (1H, s, dG-H8). It is noteworthy that, different from other deoxyguanosin-7N-yl adducts that undergo spontaneous depurination, this adduct was highly stable to the point that it could be isolated by HPLC, taken to dryness, and evaluated by NMR without depurination.

Interconversion between DHP-dA-3 and DHP-dA-4 Adducts. We found that DHP-dA-3 and DHP-dA-4 in acetonitrile/water (v/v, 1/10) are interconvertible. As analyzed by HPLC (Figure S15 in the Supporting Information), DHP-

dA-3 was converted into DHP-dA-4. After 6 days at room temperature, DHP-dA-3 and DHP-dA-4 reached an approximately equal ratio (Figure 6). Similar results were obtained starting with pure DHP-dA-4 (Figure S15 in the Supporting Information; Figure 6). It is noteworthy that in this 6 day interconversion study, neither DHP-dA-3 nor DHP-dA-4 decomposed. In contrast, interconversion did not occur between DHP-dA-1 and DHP-dA-2 (data not shown).

Interconversion between DHP-dG-3 and DHP-dG-4 Adducts. We found that DHP-dG-3 and DHP-dG-4 in acetonitrile/water (v/v, 1/10) are interconvertible at room temperature. As analyzed by HPLC, DHP-dG-3 was converted into DHP-dG-4. After 9 days, DHP-dG-3 and DHP-dG-4 reached an equal ratio (Figure 6). Similar results were obtained starting with pure DHP-dG-4 (Figure 6). Different from the DHP-dA adducts, during the 9 day interconversion study, a small part, less than 5% of DHP-dG-3 and DHP-dG-4, decomposed. In contrast, interconversion did not occur between DHP-dG-1 and DHP-dG-2 (data not shown).

Mechanism of Interconversion between DHP-dA-3 and DHP-dA-4 Adducts. For determining the mechanism by which DHP-dA-3 interconverts to DHP-dA-4 adduct, DHP-dA-3 dissolved in acetonitrile/ H_2O^{18} (v/v, 1/10) was kept at room temperature for 6 days, and then, the resulting DHP-dA-4 was collected by HPLC for LC/MS analysis. The mass spectrum of the unlabeled DHP-dA-4 (Figure 7A) had the protonated molecular ion at m/z 387 and the characteristic ions at m/z 369 ($[\text{M} - \text{H}_2\text{O} + \text{H}]^+$), m/z 253, and m/z 136, respectively. The mass spectrum of the $[\text{O}^{18}]$ DHP-dA-4 (Figure 7B) had the protonated molecular ion at m/z 389 and the characteristic ions at m/z 369 ($[\text{M} - \text{H}_2\text{O}^{18} + \text{H}]^+$), m/z 253, and m/z 138, respectively. Comparison of the molecular ions and the mass of these fragment ions as well as the assigned structures shown in

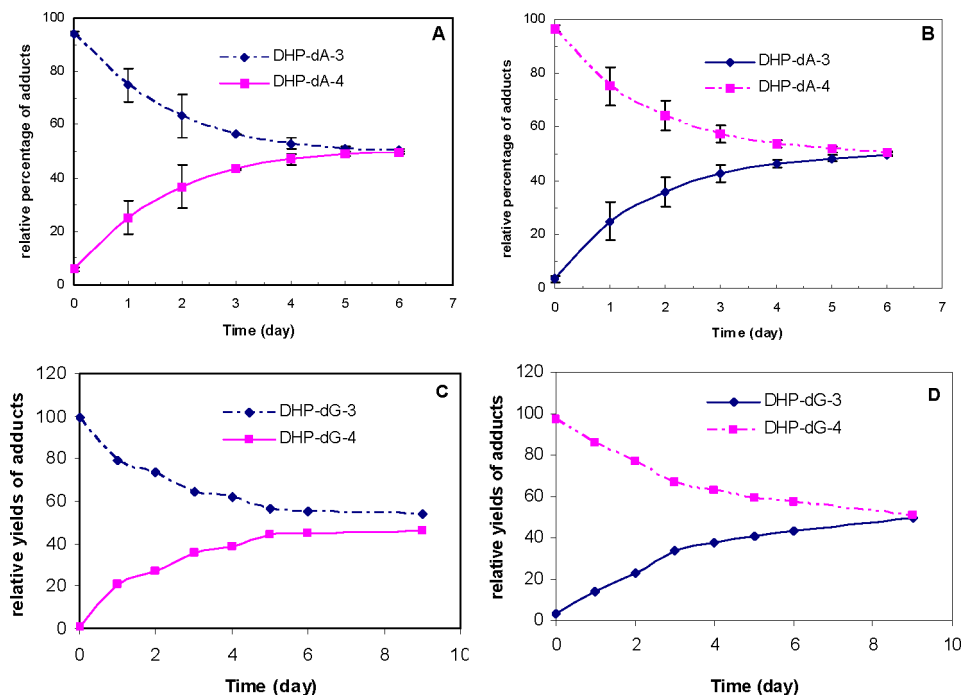


Figure 6. Interconversion between DHP-dA-3 and DHP-dA-4 in acetonitrile/water (v/v, 1/10) starting from (A) pure DHP-dA-3 and (B) pure DHP-dA-4 and interconversion between DHP-dG-3 and DHP-dG-4 in acetonitrile/water (v/v, 1/10) starting from (C) pure DHP-dG-3 and (D) pure DHP-dG-4. Data presented in this figure are means \pm SDs from three experiments. The relative percentages were calculated from their HPLC peak area ratios.

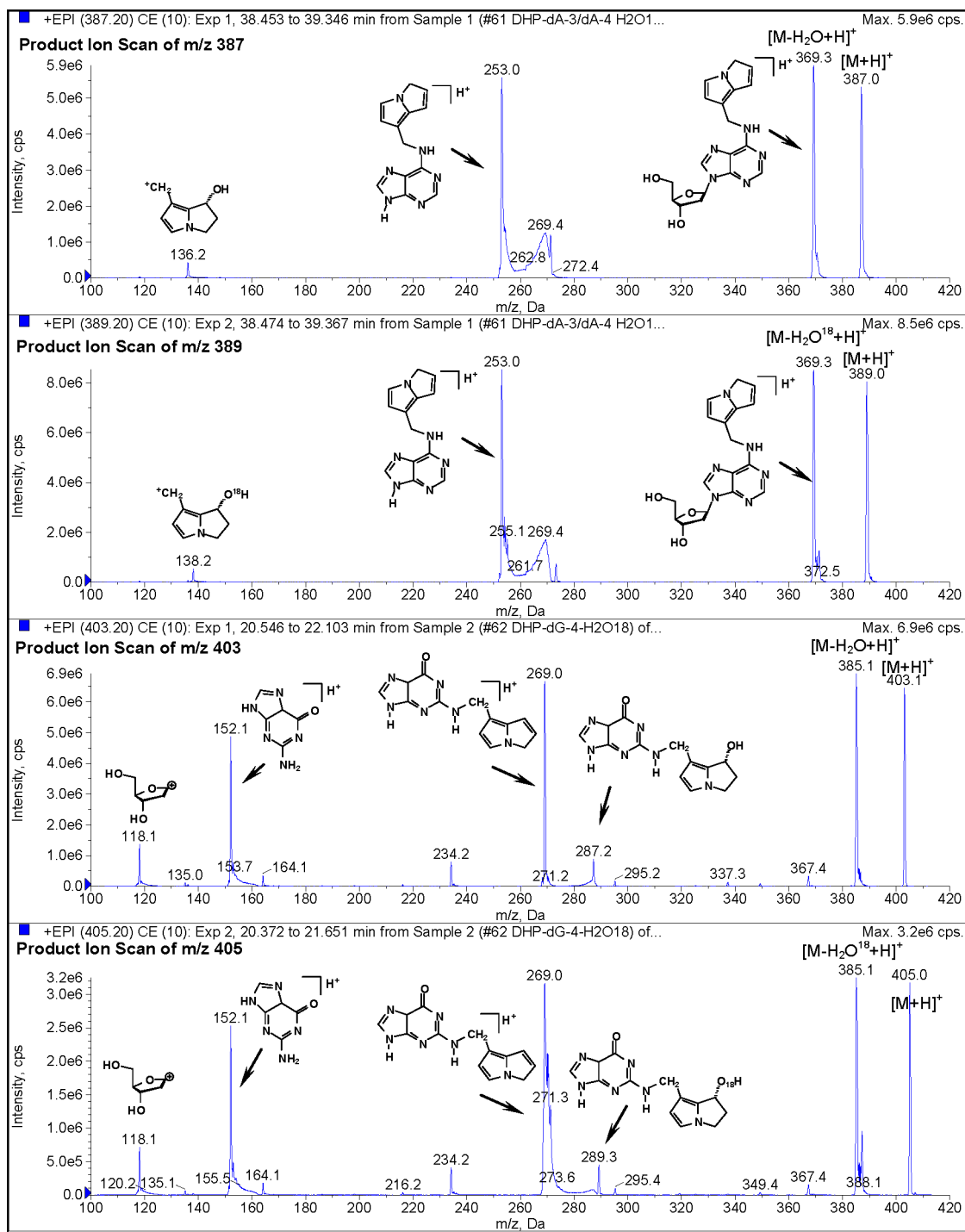


Figure 7. The LC/MS profiles of (A) DHP-dA-4, (B) $[O^{18}]$ DHP-dA-4, (C) DHP-dG-4, and (D) $[O^{18}]$ DHP-dG-4.

Figure 7A,B indicates that the O^{18} atom is specifically labeled at the 7-hydroxyl group of the necine base.

Mechanism of Interconversion between DHP-dG-3 and DHP-dG-4 Adducts. DHP-dG-3 dissolved in acetonitrile/ H_2O^{18} (v/v, 1/10) at room temperature was similarly conducted for 9 days, and the resulting $[O^{18}]$ DHP-dG-4 was collected by HPLC for LC/MS analysis. The mass spectrum of the unlabeled DHP-dG-4 (Figure 7C) had the protonated molecular ion at m/z 403 and the characteristic ions at m/z 385 ($[M - H_2O + H]^+$), m/z 287, m/z 269, m/z 152, and m/z 118 respectively. The mass spectrum of the $[O^{18}]$ DHP-dG-4

(Figure 7D) had the protonated molecular ion at m/z 405 and the characteristic ions at m/z 385 ($[M - H_2O^{18} + H]^+$), m/z 289, m/z 269, m/z 152, and m/z 118, respectively. Comparison of their mass spectra (Figure 7C,D) indicates that the O^{18} atom is specifically labeled at the 7-hydroxyl group of the necine base.

HPLC-ES-MS/MS Analysis of DHP-dG and DHP-dA Adducts Formed from Microsomal Metabolism of Riddelliine in the Presence of Calf Thymus DNA. The DHP-dG and DHP-dA adducts formed in vitro were assessed by HPLC-ES-MS/MS through multiple reaction monitoring

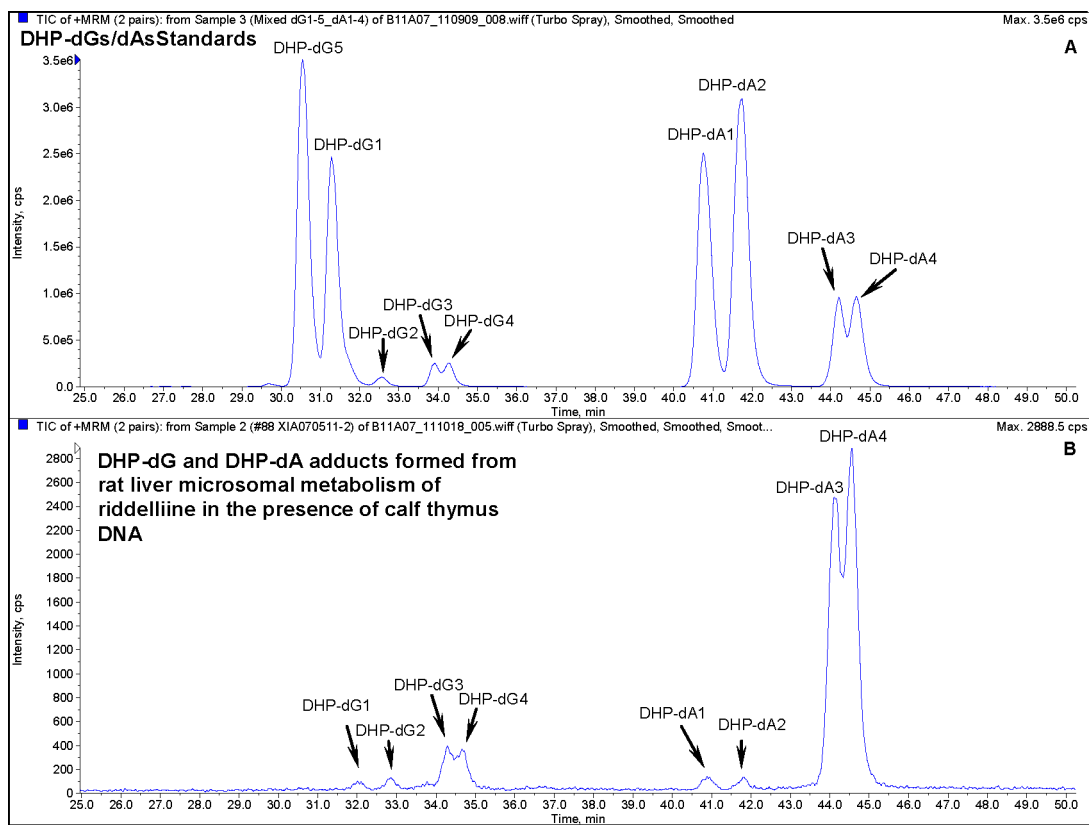


Figure 8. LC-ESI/MS/MS profiles of DHP-dG and DHP-dA adducts. (A) Chromatogram obtained using synthetic standards and (B) chromatogram obtained from *in vitro* incubation of DNA with riddelliine in the presence of rat liver microsomes.

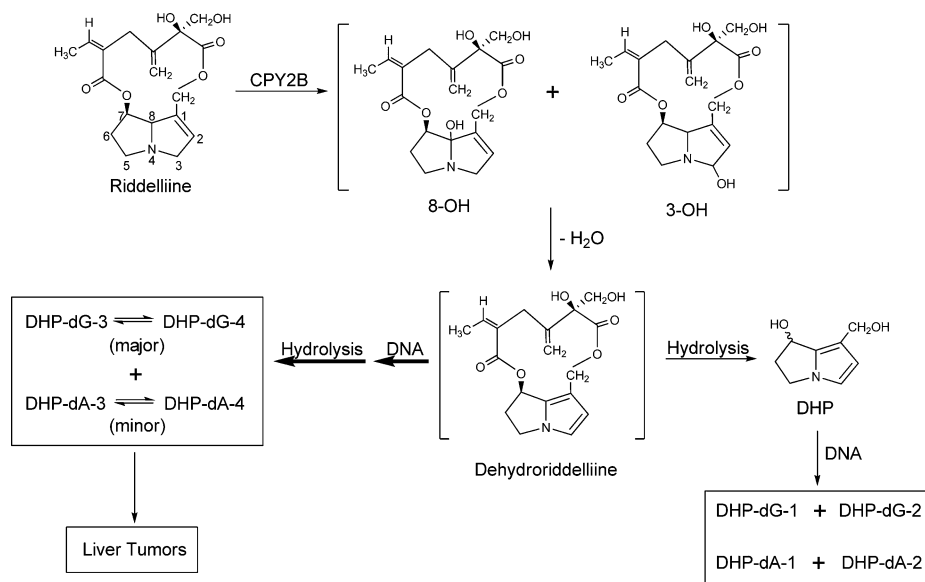


Figure 9. Proposed general mechanism leading to DHP-derived DNA adduct formation from the metabolism of riddelliine *in vivo* and *in vitro*.

(MRM). The MRM profile of the five DHP-dG adducts and the four DHP-dA adducts standards is shown in Figure 8A, and the MRM profile of the adducts formed from the metabolism is shown in Figure 8B, respectively. As the yields calculated based on their molar extinction coefficients and HPLC peak areas, these results indicate that (i) DHP-dG-1, DHP-dG-2, DHP-dG-3, and DHP-dG-4 adducts were formed, of which DHP-dG-1 and DHP-dG-2 adducts were formed to a similar extent; (ii) DHP-dG-5 adduct was not formed; (iii) DHP-dA-1, DHP-dA-

2, DHP-dA-3, and DHP-dA-4 adducts were formed predominantly, while DHP-dA-1 and DHP-dA-2 adducts were formed to a similar extent; and (iv) among all of these adducts, DHP-dA-3 and DHP-dA-4 were the most abundant, followed by DHP-dG-3 and DHP-dG-4 adducts.

DISCUSSION

In the present study, we successfully synthesized DHP-dA-3, DHP-dA-4, DHP-dG-3, and DHP-dG-4 by reaction of

dehydroriddelliine with dG and dA, respectively, for structural identification. On the basis of mass spectral, 1D ^1H NMR, 2D COSY NMR, and NOESY NMR spectral analysis, we unequivocally determined that DHP-dA-3 and DHP-dA-4 are a pair of epimers, (\pm)-7-hydroxy-9-(deoxyadenosin- N^6 -yl)-dehydrosupinidine (Scheme 1). With the same approach, we also determined that DHP-dG-3 and DHP-dG-4 are a pair of epimers (\pm)-9-(deoxyguanosin- N^2 -yl)dehydrosupinidine (Scheme 2). These structural assignments were further validated by the observation that the CD spectra of DHP-dA-3 and DHP-dA-4 are mirror images (Figure 3A) and that the CD spectra of DHP-dG-3 and DHP-dG-4 are also mirror images (Figure 3B). Thus, all of these DNA adducts were formed by the attack of the exocyclic amino group (of dG and dA) to the C9 position of the dehydroriddelliine necine base. The results indicate that the reaction of dehydroriddelliine with dG and dA is highly regioselective, with predominant binding at the C9 position of the necine base, which is in contrast to the reaction of DHR with dG and dA, predominantly producing DHP-dG-1, DHP-dG-2, DHP-dA-1, and DHP-dA-2, formed through the binding at the C7 position of the necine base.¹

There are two possible pathways that lead to DHP-derived DNA adducts from metabolism of riddelliine in vivo and in vitro.¹⁷ The first pathway is covalent binding of the dehydroriddelliine metabolite to cellular DNA, forming dehydroriddelliine-derived DNA adducts, which are subsequently hydrolyzed to DHP-derived DNA adducts. The second pathway is hydrolysis of dehydroriddelliine, catalyzed by esterases, to DHP,^{5,34–36} which subsequently binds to DNA¹⁷ (Figure 9). Because dehydropyrrolizidine alkaloid (pyrrole) metabolites are highly unstable and DHP is the most stable pyrrolic metabolite, we and other investigators^{6,17,36} previously believed that these DHP-derived DNA adducts should be preferentially formed by the second pathway rather than the first pathway. Because we found that DHP-dG-3, DHP-dG-4, DHP-dA-3, and DHP-dA-4 are the DNA adducts formed in vivo,¹ the first pathway should be predominant. On the basis of our present findings, the metabolic activation pathway of riddelliine leading to DHP-derived DNA adduct formation is hypothesized to be that illustrated in Figure 9. The metabolism of riddelliine catalyzed by P450 enzymes first generates 3-hydroxyriddelliine and/or 8-hydroxyriddelliine, which upon enzymatic dehydration produces dehydroriddelliine. Dehydroriddelliine possesses two alkylating positions at the C7 and C9 positions of the necine base capable of electrophilic reaction with cellular DNA bases in vivo. We determined that the reaction is highly regioselective, with the cellular DNA predominantly attacking to the C9 position, leading to the formation of C9-substituted DHP-DNA adducts, DHP-dG-3, DHP-dG-4, DHP-dA-3, and DHP-dA-4 (Figure 9). The secondary carbonium ion intermediate formed at the C7 position is more reactive than the primary carbonium ion formed at the C9 position of the necine base, and thus, it should preferentially form. The preferential regioselective reaction that occurred at the C9 position is apparently due to steric hindrance since the C9 position is less hindered than the C7 position.¹ Alternatively, it is also possible that the conformation of the bases in the double helix determines the positions available to the necine base.

We have also found that DHP-dG-5 was not detected in the NTP liver sample (rats dosed with riddelliine in vivo) (data not shown) or from the incubation of riddelliine with rat liver microsomes in the presence of calf thymus DNA (Figure 8).

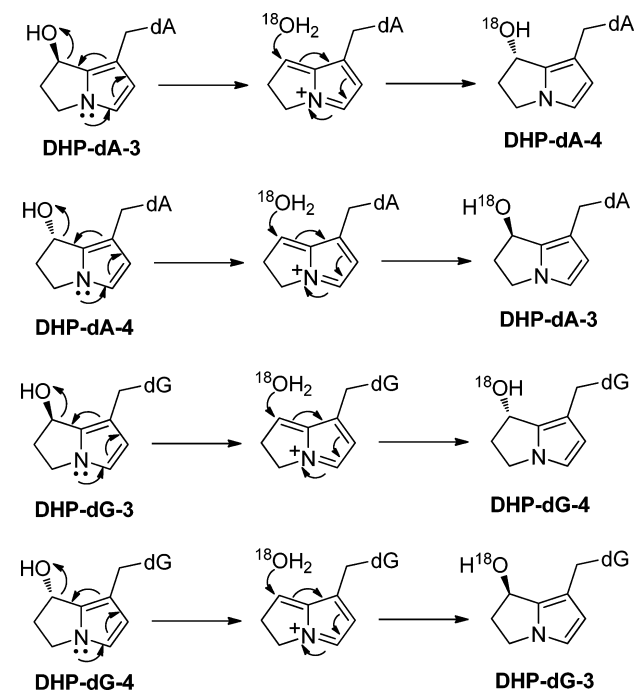
Thus, these results indicate that dehydroriddelliine preferentially binds to the exocyclic amino group, but not to the N7 position, of the dG nucleic base of the cellular DNA or the isolated calf thymus DNA.

As the structure of DHP-dG-5 was firmly determined by mass, ^1H NMR, and 2D COSY NMR spectra as DHP-dG-5, its high stability is quite different from other deoxyguanosin-7N-yl adducts that undergo spontaneous depurination. The reason for this stability warrants further investigation.

Dehydropyrrolizidine alkaloids, the primary pyrrolic metabolites, are highly unstable and biologically/chemically reactive and thus are unable to be isolated from any biological systems. Although their bindings with cellular DNA and proteins that form DNA adducts, protein adducts, and DNA–protein cross-linking adducts are responsible for hepatotoxicity, mutagenicity, and tumorigenicity of pyrrolizidine alkaloids,^{3,6,35,38,39} the structures of these resulting adducts have never been fully elucidated. Our present study represents the first report to assign unequivocally the detailed chemical structures of the DNA adducts that are responsible for the etiology of pyrrolizidine alkaloid-induced tumors. Many published reports, including ours, indicate that the most reactive site of dehydropyrrolizidine alkaloid metabolites for binding with cellular constituents is the C7 position of the necine base.^{6,17} For instance, we mistakenly synthetically prepared 3'-dGMP-DHP adducts, with the linking at the C7-position of DHP, as the authentic standards for identification and quantification of DHP-derived DNA adducts by ^{32}P -postlabeling/HPLC analysis.^{17–20,24–26,30,31,40} In our previous report using LC-ESI/MS/MS for DNA adducts analysis, we also focused on the synthesis of C7-substituted DNA adduct standards, for example, DHP-dG-1, DHP-dG-2, DHP-dA-1, and DHP-dA-2.¹ However, our present and previous studies¹ clearly show that cellular DNA, calf thymus DNA (Figure 8), dG, and dA preferentially bind to dehydropyrrolizidine alkaloid, for example, dehydroriddelliine, at the C9 position of the necine base. The drastic different regioselective reaction of these nucleophiles with DHP at the C7 position and with dehydropyrrolizidine alkaloids at the C9 position is hypothesized to be mainly because of steric hindrance at the C7 position. At present, it is not known how cellular proteins or single amino acids bind to dehydropyrrolizidine alkaloids. The only published study related to this matter is the binding of DHR with cysteine and glutathione.^{41,42} Thus, further investigation is warranted.

We have also determined that DHP-dA-3 and DHP-dA-4 are interconvertible in acetonitrile/water (v/v, 1/10) (Figure 6). DHP-dA-3 was converted into DHP-dA-4 and from DHP-dA-4 to DHP-dA-3, to reach an equal ratio in 6 days without decomposition (Figure 6). Similar interconversion occurred between DHP-dG-3 and DHP-dG-4, although the adducts decomposed to a small extent (Figure 6). We also found that in the presence of $[\text{O}^{18}]\text{H}_2\text{O}$, a fraction of the hydroxyl groups at the C7 position contained $[\text{O}^{18}]\text{OH}$, indicating that during interconversion, the OH group at the C7 position was removed from the molecule. On the basis of our findings, we propose the mechanism depicted in Scheme 3. This reaction scheme is similar to that proposed by ref 36 on the reaction of nucleophiles with the dehydropyrrolizidine alkaloids (pyrrolic metabolites), particularly the diester dehydropyrrolizidine alkaloids. While an ester group at the C7 position of the necine is a good leaving group on the nucleophilic reaction, the hydroxyl group at the C7 position is a much weaker leaving group. This is consistent with the interconversion of the DHP-

Scheme 3. Proposed Mechanism of Interconversion between DHP-dA-3 and DHP-dA-4 and between DHP-dG-3 and DHP-dG-4



dA and DHP-dG adducts requiring 6 and 9 days, respectively, to reach an equal ratio of both epimers, DHP-dA-3 and DHP-dA-4, as well as DHP-dG-3 and DHP-dG-4 (Scheme 3).

In summary, we have fully elucidated the structures of DHP-dG-3, DHP-dG-4, DHP-dA-3, and DHP-dA-4. They are the DNA adducts formed *in vivo*, and the level of their formation correlates with the tumor potency in liver of rats administered with riddelliine. Thus, we propose that these DNA adducts are potential DNA biomarkers of pyrrolizidine alkaloid-induced tumorigenicity as well as pyrrolizidine alkaloid exposure.

■ ASSOCIATED CONTENT

Supporting Information

Figures S1–S15. This material is available free of charge via the Internet at <http://pubs.acs.org>.

■ AUTHOR INFORMATION

Corresponding Author

*Tel: +1-870-543-7207. Fax: +1-870-543-7136. E-mail: peter.fu@fda.hhs.gov.

Funding

This research was supported in part by appointment (Y.Z.) to the Postgraduate Research Program at the NCTR administered by the Oak Ridge Institute for Science and Education through an interagency agreement between the U.S. Department of Energy and the FDA.

Notes

This article is not an official U.S. Food and Drug Administration (FDA) guidance or policy statement. No official support or endorsement by the U.S. FDA is intended or should be inferred.

The authors declare no competing financial interest.

■ ACKNOWLEDGMENTS

We thank Dr. Po-Chuen Chan of NTP for supplying riddelliine and Frederick A. Beland for critical review of this manuscript.

■ ABBREVIATIONS

CD, circular dichroism spectroscopy; DHR, dehydroretronecine or (–)-*R*-6,7-dihydro-7-hydroxy-1-hydroxymethyl-5*H*-pyrrolizine; DHP, (±)-6,7-dihydro-7-hydroxy-1-hydroxymethyl-5*H*-pyrrolizine; PNK, cloned T4 polynucleotide kinase; MN, micrococcal nuclease; SPD, spleen phosphodiesterase; dG, 2'-deoxyguanosine; dA, 2'-deoxyadenosine; DHP-dG-1 and DHP-dG-2, epimeric pairs of 7-(deoxyguanosin-*N*²-yl)-dehydrosupinidine; DHP-dG-3 and DHP-dG-4, epimeric pairs of 7-hydroxy-9-(deoxyguanosin-*N*²-yl)dehydrosupinidine; DHP-dG-5, 7-hydroxy-9-(deoxyguanosin-7*N*-yl)dehydrosupinidine; DHP-dA-1 and DHP-dA-2, epimeric pairs of 7-(deoxyadenosin-*N*⁶-yl)dehydrosupinidine; DHP-dA-3 and DHP-dA-4, 7-hydroxy-9-(deoxyadenosin-*N*⁶-yl)-dehydrosupinidine; LC-ESI-MS/MS, high-performance liquid chromatography electrospray ionization tandem mass spectrometry; NCTR, National Center for Toxicological Research; NTP, National Toxicology Program

■ REFERENCES

- (1) Fu, P. P., Chou, M. W., Churchwell, M., Wang, Y., Zhao, Y., Xia, Q., Gamboa da Costa, G., Marques, M. M., Beland, F. A., and Doerge, D. R. (2010) High-performance liquid chromatography electrospray ionization tandem mass spectrometry for the detection and quantitation of pyrrolizidine alkaloid-derived DNA adducts *in vitro* and *in vivo*. *Chem. Res. Toxicol.* 23, 637–652.
- (2) Fu, P. P., Xia, Q., Chou, M. W., and Lin, G. (2007) Detection, hepatotoxicity, and tumorigenicity of pyrrolizidine alkaloids in Chinese herbal plants and herbal dietary supplements. *J. Food Drug Anal.* 15, 400–415.
- (3) Fu, P. P., Xia, Q., Lin, G., and Chou, M. W. (2004) Pyrrolizidine alkaloids—Genotoxicity, metabolism enzymes, metabolic activation, and mechanisms. *Drug Metab. Rev.* 36, 1–55.
- (4) Fu, P. P., Yang, Y.-C., Xia, Q., Chou, M. W., Cui, Y., and Lin, G. (2002) Pyrrolizidine alkaloids—Tumorigenic components in Chinese herbal medicines and dietary supplements. *J. Food Drug Anal.* 10, 198–211.
- (5) IPCS (1989) Pyrrolizidine Alkaloids Health and Safety Guides. *Health and Safety Criteria Guides* 26, WHO, Geneva, Switzerland.
- (6) Mattocks, A. R. (1986) *Chemistry and Toxicology of Pyrrolizidine Alkaloids*, Academic Press, London, NY.
- (7) Roeder, E. (1995) Medicinal plants in Europe containing pyrrolizidine alkaloids. *Pharmazie* 50, 83–98.
- (8) Roeder, E. (2000) Medicinal plants in China containing pyrrolizidine alkaloids. *Pharmazie* 55, 711–726.
- (9) Roeder, E., and Wiedenfeld, H. (2009) Pyrrolizidine alkaloids in medicinal plants of Mongolia, Nepal and Tibet. *Pharmazie* 64, 699–716.
- (10) Smith, L. W., and Culvenor, C. C. (1981) Plant sources of hepatotoxic pyrrolizidine alkaloids. *J. Nat. Prod.* 44, 129–152.
- (11) Betz, J. M., Eppley, R. M., Taylor, W. C., and Andrzejewski, D. (1994) Determination of pyrrolizidine alkaloids in commercial comfrey products (*Symphytum* sp.). *J. Pharm. Sci.* 83, 649–653.
- (12) Edgar, J. A., Roeder, E., and Molyneux, R. J. (2002) Honey from plants containing pyrrolizidine alkaloids: a potential threat to health. *J. Agric. Food Chem.* 50, 2719–2730.
- (13) Huxtable, R. J., Ed. (1989) *Human Health Implications of Pyrrolizidine Alkaloids and Herbs Containing them*, Vol. 1, CRC Press Inc., Boca Raton, FL.
- (14) Stegelmeier, B. L., Edgar, J. A., Colegate, S. M., Gardner, D. R., Schoch, T. K., Coulombe, R. A., and Molyneux, R. J. (1999)

Pyrrrolizidine alkaloid plants, metabolism and toxicity. *J. Nat. Toxins* 8, 95–116.

(15) Cook, J. W., Duffy, E., and Schoental, R. (1950) Primary liver tumours in rats following feeding with alkaloids of *Senecio jacobaea*. *Br. J. Cancer* 4, 405–410.

(16) Schoental, R., head, M. A., and Peacock, P. R. (1954) Senecio alkaloids: Primary liver tumours in rats as a result of treatment with (1) a mixture of alkaloids from *S. jacobaea* lin.; (2) retrorsine; (3) isatidine. *Br. J. Cancer* 8, 458–465.

(17) Yang, Y. C., Yan, J., Doerge, D. R., Chan, P. C., Fu, P. P., and Chou, M. W. (2001) Metabolic activation of the tumorigenic pyrrrolizidine alkaloid, riddelliine, leading to DNA adduct formation in vivo. *Chem. Res. Toxicol.* 14, 101–109.

(18) Chou, M. W., Jian, Y., Williams, L. D., Xia, Q., Churchwell, M., Doerge, D. R., and Fu, P. P. (2003) Identification of DNA adducts derived from riddelliine, a carcinogenic pyrrrolizidine alkaloid. *Chem. Res. Toxicol.* 16, 1130–1137.

(19) Chou, M. W., Yan, J., Nichols, J., Xia, Q., Beland, F. A., Chan, P. C., and Fu, P. P. (2003) Correlation of DNA adduct formation and riddelliine-induced liver tumorigenesis in F344 rats and B6C3F(1) mice. *Cancer Lett.* 193, 119–125.

(20) Xia, Q., Chou, M. W., Kadlubar, F. F., Chan, P. C., and Fu, P. P. (2003) Human liver microsomal metabolism and DNA adduct formation of the tumorigenic pyrrrolizidine alkaloid, riddelliine. *Chem. Res. Toxicol.* 16, 66–73.

(21) Chan, P. C., Haseman, J. K., Prejean, J. D., and Nyska, A. (2003) Toxicity and carcinogenicity of riddelliine in rats and mice. *Toxicol. Lett.* 144, 295–311.

(22) National Toxicology Program (2011) NTP 12th Report on Carcinogens. *Rep. Carcinog.* 12, iii–499.

(23) Chou, M. W., and Fu, P. P. (2006) Formation of DHP-derived DNA adducts in vivo from dietary supplements and chinese herbal plant extracts containing carcinogenic pyrrrolizidine alkaloids. *Toxicol. Ind. Health* 22, 321–327.

(24) Wang, Y. P., Fu, P. P., and Chou, M. W. (2005) Metabolic activation of the tumorigenic pyrrrolizidine alkaloid, retrorsine, leading to DNA adduct formation in vivo. *Int. J. Environ. Res. Public Health* 2, 74–79.

(25) Wang, Y. P., Yan, J., Beger, R. D., Fu, P. P., and Chou, M. W. (2005) Metabolic activation of the tumorigenic pyrrrolizidine alkaloid, monocrotaline, leading to DNA adduct formation in vivo. *Cancer Lett.* 226, 27–35.

(26) Xia, Q., Chou, M. W., Edgar, J. A., Doerge, D. R., and Fu, P. P. (2006) Formation of DHP-derived DNA adducts from metabolic activation of the prototype heliotridine-type pyrrrolizidine alkaloid, lasiocarpine. *Cancer Lett.* 231, 138–145.

(27) Xia, Q., Chou, M. W., Lin, G., and Fu, P. P. (2004) Metabolic formation of DHP-derived DNA adducts from a representative otonecine type pyrrrolizidine alkaloid clivorine and the extract of *Ligularia hodgsonnii* hook. *Chem. Res. Toxicol.* 17, 702–708.

(28) Xia, Q., Yan, J., Chou, M. W., and Fu, P. P. (2008) Formation of DHP-derived DNA adducts from metabolic activation of the prototype heliotridine-type pyrrrolizidine alkaloid, heliotrine. *Toxicol. Lett.* 178, 77–82.

(29) Yan, J., Nichols, J., Yang, Y. C., Fu, P. P., and Chou, M. W. (2002) Detection of riddelliine-derived DNA adducts in blood of rats fed riddelliine. *Int. J. Mol. Sci.* 3, 1019–1026.

(30) Yan, J., Xia, Q., Chou, M. W., and Fu, P. P. (2008) Metabolic activation of retronecine and retronecine N-oxide—Formation of DHP-derived DNA adducts. *Toxicol. Ind. Health* 24, 181–188.

(31) Yang, Y., Yan, J., Churchwell, M., Beger, R., Chan, P., Doerge, D. R., Fu, P. P., and Chou, M. W. (2001) Development of a ³²P-postlabeling/HPLC method for detection of dehydroretronecine-derived DNA adducts in vivo and in vitro. *Chem. Res. Toxicol.* 14, 91–100.

(32) Mattocks, A. R., Jukes, R., and Brown, J. (1989) Simple procedures for preparing putative toxic metabolites of pyrrrolizidine alkaloids. *Toxicol.* 27, 561–567.

(33) Zhao, Y., Xia, Q., Yin, J. J., Lin, G., and Fu, P. P. (2011) Photoirradiation of dehydropyrrrolizidine alkaloids—Formation of reactive oxygen species and induction of lipid peroxidation. *Toxicol. Lett.* 205, 302–309.

(34) IARC (1976) Pyrrrolizidine Alkaloids. In *IARC Monograph on the Evaluation of Carcinogenic Risk of Chemicals to Man—Some Naturally Occurring Substances*, Vol. 10, International Agency for Research in Cancer, Lyon, France.

(35) Kim, H. Y., Stermitz, F. R., Li, J. K., and Coulombe, R. A., Jr. (1999) Comparative DNA cross-linking by activated pyrrrolizidine alkaloids. *Food Chem. Toxicol.* 37, 619–625.

(36) Mattocks, A. R. (1968) Toxicity of pyrrrolizidine alkaloids. *Nature* 217, 723–728.

(37) Galloway, S. M., Armstrong, M. J., Reuben, C., Colman, S., Brown, B., Cannon, C., Bloom, A. D., Nakamura, F., Ahmed, M., Duk, S., et al. (1987) Chromosome aberrations and sister chromatid exchanges in Chinese hamster ovary cells: Evaluations of 108 chemicals. *Environ. Mol. Mutagen.* 10 (Suppl. 10), 1–175.

(38) Hincks, J. R., Kim, H. Y., Segall, H. J., Molyneux, R. J., Stermitz, F. R., and Coulombe, R. A. (1991) DNA cross-linking in mammalian cells by pyrrrolizidine alkaloids: structure-activity relationships. *Toxicol. Appl. Pharmacol.* 111, 90–98.

(39) Kim, H. Y., Stermitz, F. R., and Coulombe, R. A. (1995) Pyrrrolizidine alkaloid-induced DNA-protein cross-links. *Carcinogenesis* 16, 2691–2697.

(40) Fu, P. P., Chou, M. W., Xia, Q., Yang, Y. C., Yan, J., Doerge, D. R., and Chan, P. C. (2001) Genotoxic pyrrrolizidine alkaloids and pyrrrolizidine alkaloid N-oxides - mechanisms leading to DNA adduct formation and tumorigenicity. *Environ. Carcinogen. Ecotoxicol. Rev.* 19, 353–386.

(41) Mattocks, A. R., and Jukes, R. (1990) Recovery of the pyrrolic nucleus of pyrrrolizidine alkaloid metabolites from sulphur conjugates in tissues and body fluids. *Chem.-Biol. Interact.* 75, 225–239.

(42) Robertson, K. A., Seymour, J. L., Hsia, M. T., and Allen, J. R. (1977) Covalent interaction of dehydroretronecine, a carcinogenic metabolite of the pyrrrolizidine alkaloid monocrotaline, with cysteine and glutathione. *Cancer Res.* 37, 3141–3144.